RESEARCH PAPER

# Lewis acid catalyzed novel one-pot multicomponent production of pyridine analogues and its antidiabetic studies

**Perumal Gobinath[1*], Vadivel Ambigai[2], Rajasekar M[3], Kavitha J[4] and Madhan Kumar S[5]**

[*1]Department of Chemistry, V.S.B. Engineering College, Karur, Tamil Nadu, India – 639111.
Email ID: gopi10207005@gmail.com ,Orcid ID:0009-0003-2391-4382
[2]Department of Chemistry, Jai Shriram Engineering College, Tirupur, Tamil Nadu, India – 638660.
Email ID: ambigaivadivelsh@jayshriram.edu.in
[3]Department of Chemistry, K.S.R. College of Engineering, Namakkal, Tamil Nadu, India - 637215.
Email ID: rjsekar56@gmail.com
[4]Department of Chemistry, Jai Shriram Engineering College, Tirupur, Tamil Nadu, India – 638660.
Email ID: kavithajchem@gmail.com
[5]Department of Chemistry, Erode Sengunthar Engineering College, Erode, Tamil Nadu, India – 638057.
Email ID: madhansangaiya@gmail.com

**ABSTRACT**

The global prevalence of diabetes mellitus (DM) is steadily increasing, posing a significant public health challenge. DM is categorized into two basic types: Type I (TYDM-1) and Type II (TYDM-2). TYDM-I is characterized by an absolute absence of insulin synthesis, whereas TYDM-II is distinguished by peripheral tissue resistance to insulin action and insufficient compensatory insulin secretion. Chronic hyperglycemia associated with diabetes leads to malfunction in the cardiovascular, neurological, renal, and ocular systems. A variety of pharmaceutical types are being used in diabetic care, each associated with differing levels of side effects. Therefore, it is crucial to develop new treatment agents with improved efficacy and safety profiles. A streamlined, one-pot, multi-component fabrication of pyridine analogues (**1-1c**) and (**2-2a**) is presented. A combination of 2-aminopyridine, 3-nitrobenzaldehyde, and tertiary butyl isocyanide in an ethanolic media yielded the aforementioned compounds in high quantities. This synthesis process included a number of Lewis acids as catalysts. The synthesized compounds (**1-1c**) and (**2-2a**) were validated through various spectroscopic approaches, including Nuclear Magnetic Resonance spectroscopy ($^{1}$H & $^{13}$C NMR), Fourier Transform Infrared Spectroscopy (FT-IR), High Resolution Mass Spectroscopy (HR-MS), Ultra Violet-Visible spectroscopy (UV-Vis), and elemental analysis. The newly synthesized analogues (**1-1c**) and (**2-2a**) were subsequently assessed for antidiabetic properties. Of the synthesized compounds (**1-1c**) and (**2-2a**), compounds **1a** and **1c** exhibited superior antioxidant and antidiabetic properties.

**Keywords:** 2-aminopyridine; Benzaldehyde; Isocyanide; Imidazopyridine; Spectroscopy

**How to cite this article:** Gobinath P, Ambigai V, Rajasekar M, Kavitha J, Madhan Kumar S. Lewis Acid Catalyzed Novel One-Pot Multicomponent Production of Pyridine Analogues and Its Antidiabetic Studies. Int J Drug Deliv Technol. 2026;16(72s): 801-817. DOI: 10.25258/ijddt.16.72s.89

**Source of support:** Nil.

**Conflict of interest:** None

## INTRODUCTION

Endocrinal and metabolic problems, generally referred to as type 2 diabetes mellitus (T2DM), affect about 370 million adults worldwide. T2DM is attributed to inadequate insulin secretion or insulin resistance. T2DM is associated with several medical conditions, such as hyperuricemia, cardiac disease, hyperlipidaemia, and conceivably fatal consequences, with a higher blood sugar level [3]. Acarbose and other established α-glucosidase and α-amylase inhibitors successfully reduce postprandial blood glucose levels in individuals with diabetes. A multitude of pharmaceuticals has been produced to manage diabetes. Enzymes that hydrolyse starch into glucose, like α-glucosidase and α-amylase, are essential for the regulation of blood glucose levels. Inhibitors of α-glucosidase and α-amylase might impede this process, hence reducing the quantity of glucose absorbed [4]. Consequently, several researchers are increasingly concentrating on the discovery of new α-amylase and α-glucosidase inhibitors [5-9].

Multi-component reactions (MCRs) have emerged as a powerful tool in modern engineered organic chemistry, owing to their beneficial attributes such as atom efficiency, streamlined reaction processes, and the ability to produce molecules of interest by integrating diverse compounds in one chemical synthesis phenomenon. The purifying of the substances obtained from MCRs is often uncomplicated, since all organic substrates utilized must be entirely utilized and incorporated into the target compound [11-13]. MCRs, yielding compelling heterocyclic structures, are particularly beneficial for the development of diverse chemical libraries of pharmaceutical molecules.

Functional heterocyclic structures based on imidazo [1,2-a] pyridines have significant pharmaceutical

*Author for Correspondence: (Perumal Gobinath & gopi10207005@gmail.com

applications, especially the treatment of heart disease, headaches, gastric ailments, and antiviral therapy, particularly anti-HIV treatments [14-18]. The principal pharmacological use of imidazo[1,2-a]pyridines is the administration of zolpidem (**1**) for the management of sleeplessness. Comparable imidazo[1,2-a]pyridines include the previously used anticonvulsant alpidem (**2**) [19], as well as the functionally related compounds necopidem (**3**) [20] and saripidem (**4**) [20] (Figure 1), that possess sedative and anxiolytic properties. The imidazo[1,2-a]pyridine molecule GSK812397 is now under investigation for HIV treatment [21-23]. Furthermore, imidazo[1,2-a]pyridines have significant effectiveness as anti-infectious agents, receptor ligands, and enzyme antagonists [24]. As a result, imidazo[1,2-a]pyridines are occasionally known as "advantageous drugs."

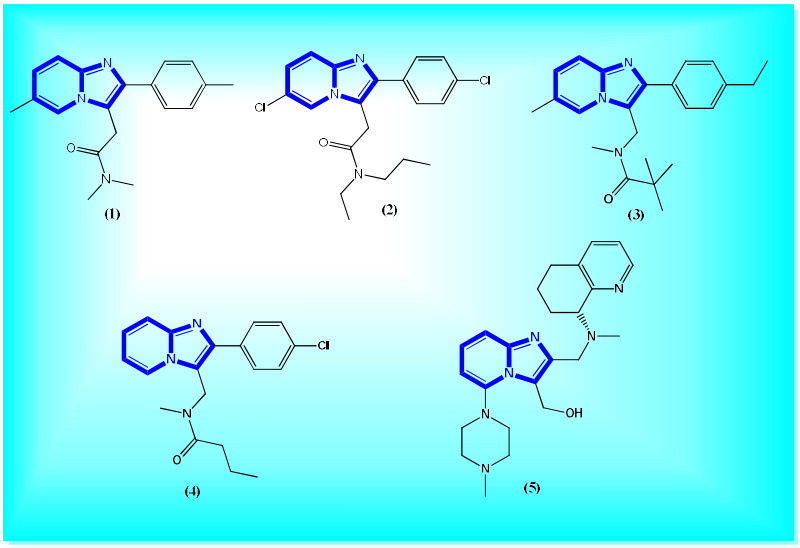


**Figure 1. Biologically active imidazo[1,2-a]pyridines**

Imidazo-[1,2-a]-pyridines are often produced by the reaction of 2-amino pyridine with α-halocarbonyl substances [25-27]. The Groebke-Blackburn-Bienaymé multicomponent conversion procedure has emerged as a predominant method for producing imidazo[1,2-a]pyridines [28]. This method enables a single-pot of transformed imidazo[1,2-a]pyridines using modified isocyanides, aldehydes, and 2-aminopyridines, often using an acid catalyst such as Montmorillonite K-10 clay, scandium triflate, or zinc(II) chloride [29,30]. This study describes a Lewis acid-catalyzed one-pot three-component fabrication of imidazo[1,2-a]pyridine derivatives utilizing 2-amino pyridine, isocyanide, and aldehydes in an alcohol-based solvents. The imidazo[1,2-a]pyridine derivatives (1a-c) and (2-2a) were further assessed for antidiabetic properties.

## MATERIALS AND METHODS

### Chemistry

All studies used ethanol (analytical reagent grade) and double-distilled water. All substances for production were acquired from reputable vendors and employed devoid of additional purifying. Absorption spectra were recorded on SPECORD 200 PLUS and Cary 50 Bio UV-visible spectrophotometer. NMR spectra were recorded using a Bruker Advance 400 MHz spectrometer operated at 400 MHz. The ESI-HRMS spectrum was acquired using a Thermoexactive PE Sciex API3000 mass spectroscopy. Melting points were obtained using transparent glassy capillary utilizing Stuart scientific SMP3 equipment and are unaltered. Chemical shifts are expressed in parts per million (ppm). The pureness of the analysed substances was determined using elemental analyses. The fundamental examination (C, H, and N) of the desired substances deviates by ± 0.4% from the estimated values.

**General method for the production of imidazole-pyridine analogue (1)**

5-chloro-2-aminopyridine (0.94 g, 10 mmol), tert-butyl isocyanide (1.2 g, 10 mmol), 4-Nitrobenzaldehyde (1.5 g, 10 mmol), and ethanol (20 ml) were introduced into a 100 ml round-bottom flask. An iodide catalyst (0.5 mol) was introduced, and the reaction mixture was agitated at ambient temperature. The reaction's progression was assessed by thin-layer chromatography (TLC). A precipitate of orange-yellow hue was generated. Upon termination of the aforementioned reaction, the resultant precipitate was filtrated, rinsed using sufficient ethanol, and dried under vacuum conditions. Successfully obtained the precipitate and crystals from ethanol, achieving a 93% yield, and proceeded to analyse the subsequent spectral information.

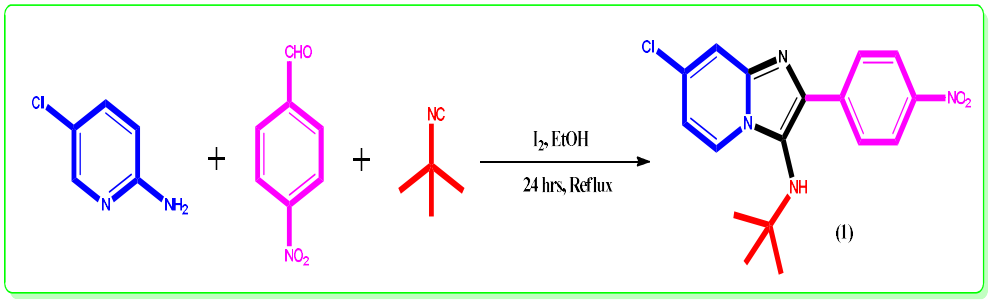


**Scheme 1. Schematic illustration of the production of compound (1)**

**General method for the production of imidazole-pyridine analogue (1a)**

1 g of the substance (1) was placed in 12 mL of hydrochloric acid (6 equivalents) and placed in a 100 mL round-bottom flask, then stirred briskly to achieve a homogenous solution. Two equivalents of Sn were incorporated into the reaction mixture, which was then refluxed in a water bath at 65°C for 40-50 minutes. Following this, the resulting mixture underwent cooling to ambient temperature, and the addition of NaOH solution resulted in precipitation. An additional base was used to eliminate excess Tin (Sn); thereafter, the organic portion was derived with ethyl acetate and water. The organic layer was then evaporated under decreased pressure to provide the aforementioned compound 1a.

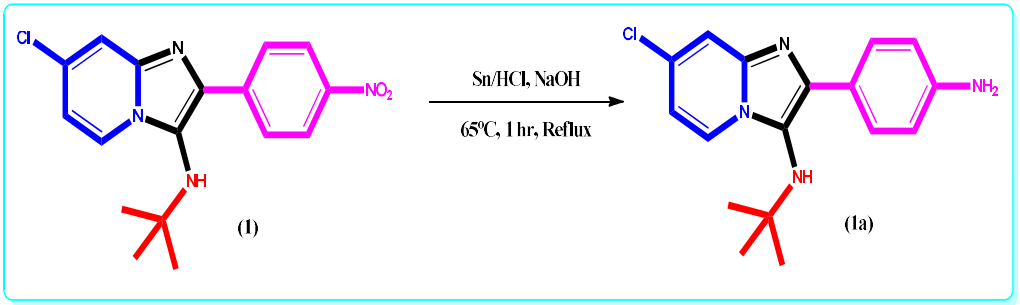


**Scheme 2. Schematic illustration of the production of compound (1a)**

**General method for the production of imidazole-pyridine analogue (1b)**

Two hundred milligrams of compound (1) was placed in 9 ml of TFA and 1 ml of water, thereafter underwent refluxing at 70°C for 16 to 17 hours. The resulting solution was analyzed using thin-layer chromatography (TLC). The complete reaction mixture was evaporated under reduced pressure to get a light brown solid outcome of a compound (1b).

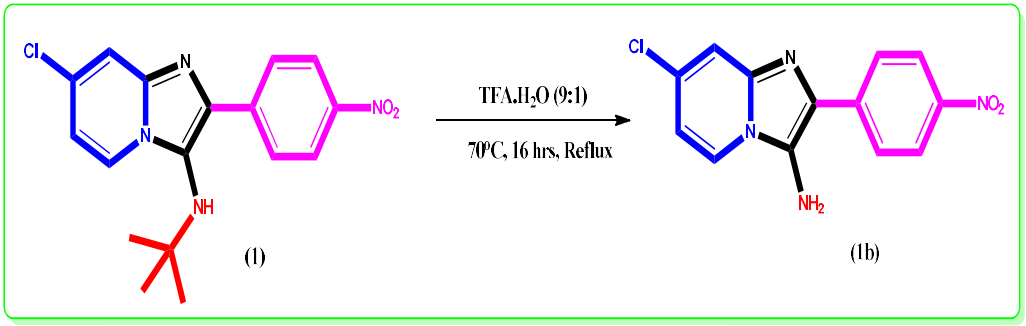


**Scheme 3. Schematic illustration of the production of compound (1b)**

**General method for the production of imidazole-pyridine analogue (1c)**

1 g of the component (1b, 6 equivalents) was immersed in 12 mL of hydrochloric acid and transferred to a 100 mL round-bottom flask, where it was agitated briskly to achieve a homogenous solution. To the reaction mixture, 2 equivalents of Sn were introduced and the entire solution underwent refluxing at 65°C. Around 40-50 minutes, the reaction mixture was chilled to ambient temperature, and NaOH solution was added in order to produce the intended product. Subsequently, more NaOH solution was used to eliminate excess Tin (Sn); thereafter, the organic layer was taken out utilizing ethyl acetate and water. The organic layer was subsequently evaporated over reduced pressure to provide product 1c.

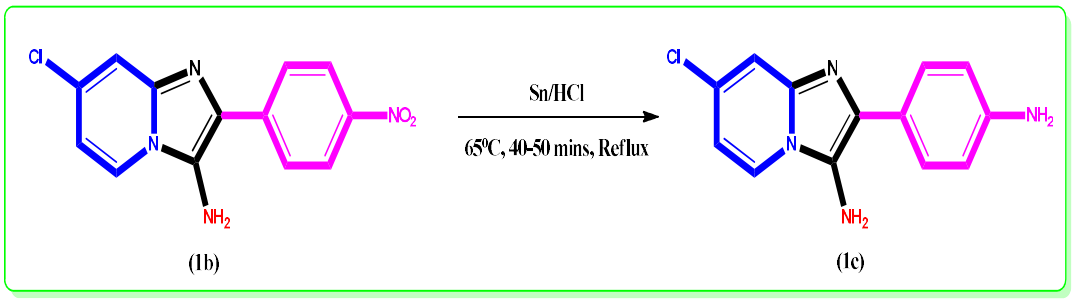


**Scheme 4. Schematic illustration of the production of compound (1c)**

**General method for the production of imidazole-pyridine analogue (2)**

5-chloro-2-aminopyridine (0.94g, 10 mmol), tertiary butyl isocyanide (1.24 g, 10 mmol), N-dimethyl benzaldehyde (1.5 g, 10 mmol), and ethanol (20 mL) were introduced into a 100 mL round-bottom flask. 0.5 mol of iodide was incorporated and the subsequent solution was agitated at ambient temperature. The reaction's progression was assessed by thin-layer chromatography (TLC). A lemon-yellow residue was produced. Upon termination of the process, precipitated material was filtrated, rinsed with excessive ethanol, and subsequently dried under vacuum conditions. Successfully obtained the white residue. The synthetic production pathway of compound 2 is shown in Scheme 5.

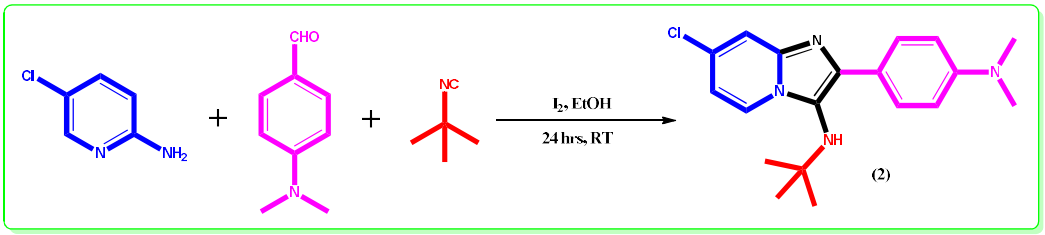


**Scheme 5. Schematic illustration of the production of compound (2)**

**General method for the production of imidazole-pyridine analogue (2a)**

200 mg of component (2) were submerged in 9 ml of trifluoroacetic acid (TFA) and 1 ml of water subsequently underwent refluxing at 70°C for 16 to 17 hours. The reaction combination was analyzed using thin-layer chromatography (TLC). The resultant mixture was evaporated under reduced pressure to provide a light brown residue of component 2a. The synthetic pathway of chemical 2a is shown in Scheme 6.

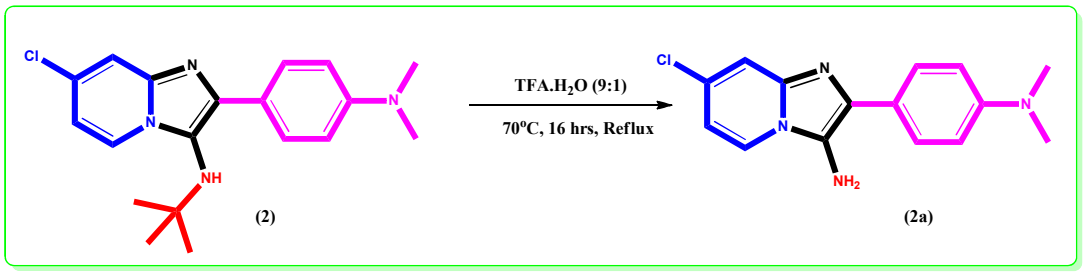


**Scheme 6. Schematic illustration of the production of compound (2a)**

**Antidiabetic effect**

**α-Amylase inhibitory action**

The α-amylase inhibition effect was assessed utilizing the approaches already reported [31]. Five hundred microliters of the test specimen (125-500 uM) and five hundred microliters of 0.5 mg/mL α-amylase substrate mixture (derived from Aspergillus oryzae) in 0.2 mM phosphate buffer were placed in an incubator for ten minutes at 25 ºC. Subsequent to pre-treatment, 500 µL of a 1% starch solution in 0.02 M sodium phosphate buffer was introduced and maintained for 10 minutes at 25 °C. One milliliter of DNS coloring agent was utilized to terminate the process. The mixture were thereafter immersed in hot water for 5 minutes earlier being allowed to cool to the ambient temperature. Following the dilution of the mixture with 10 mL of distilled water, the absorbance at 540 nm was recorded. The acarbose was used as a positive control [32]. The % of enzyme inhibition was determined utilizing the below relation:

**% of α-amylase Inhibitory effect = (Absorbance of control – Absorbance of compound) / Absorbance of control x 100 (1)**

**α-Glucosidase inhibitory action**

The inhibition of α-glucosidase efficiency was assessed employing an amended version of an established technique [33]. In 50 mL of phosphate buffer comprising 100 mg of BSA, 1 mg of α-glucosidase was solubilized. The reaction mixture comprised of 5 µL of samples at varying dosages (125 - 1000 uM), 250 µL of 5 mM p-nitrophenyl-D-glucopyranoside, and 490 µL of phosphate buffer. Following a 5-minute pretreatment period at 37 ºC, 200 µL of α-glucosidase was introduced and maintained at 37 ºC for 15 minutes. The entire process was ended by the addition of 1000 µL of 100 mM $Na_2CO_3$. The activity of α-glucosidase was quantified utilizing a UV-Vis spectrophotometer at 400 nm. Acarbose was utilized as a standard for the α-glucosidase inhibitor [34].

**Statistical analysis**

All experiments were conducted in triplicate, and the results are presented as mean ± standard deviation (SD). Data analysis was performed using Microsoft Excel (Microsoft Corporation, Redmond, WA, USA). The $IC_{50}$ values were estimated by plotting the percentage inhibition against the logarithm of sample concentration and applying linear regression analysis to the linear portion of the dose–response curve. The $IC_{50}$ was calculated from the regression equation corresponding to 50% inhibition. The quality of the regression model was assessed using the coefficient of determination ($R^2$). Differences were considered statistically significant at $p < 0.05$.

## RESULTS AND DISCUSSION

**N-(tert-butyl)-2-(4-nitrophenyl)imidazo[1,2-a]pyridin-3-amine (1)**

Orange-yellowish solid; Yield: 93%; FT-IR (KBr, $cm^{-1}$): 3350 (NH); UV-Vis ($\lambda_{Max}$): 368 nm; $^1H$ NMR (400 MHz, $CDCl_3$) δ 8.25 (s, 1H), 8.18 (d, J = 6.9 Hz, 2H), 7.54 (s, 2H), 7.21 (t, 1H), 4.82 (t, 1H), 3.08 (s, 1H), 1.09 (s, 9H); $^{13}C$ NMR (101 MHz, $CDCl_3$) δ 146.62, 142.54, 141.99, 137.08, 128.39, 125.01, 124.88, 123.54, 123.41, 117.70, 112.02, 77.40, 77.08, 76.76, 56.79, 30.48; Mass calculated for $C_{17}H_{18}N_4O_2$: ESI (m/z) = 310.15 found 311.20 $(M + H)^+$; Elemental analysis: Anal. Calcd. for $C_{17}H_{18}N_4O_2$: C, 65.79; H, 5.85; N, 18.05 %; Found: C, 65.76; H, 5.83; N, 18.07 %.

**2-(4-aminophenyl)-N-(tert-butyl)imidazo[1,2-a]pyridin-3-amine (1a)**

Brown solid; Yield: 93%; FT-IR (KBr, $cm^{-1}$): 3315 (NH); UV-Vis ($\lambda_{Max}$): 370 nm; $^1H$ NMR (400 MHz, $CDCl_3$) δ 8.25 – 8.17 (s, 1H), 7.76 – 7.67 (d, 2H), 7.53 – 7.44 (d, 1H), 7.09 (t, J = 8.9, 6.7, 1.4 Hz, 1H), 6.78 – 6.70 (D, 3H), 3.27 (s, 3H), 1.05 (S, J = 2.8 Hz, 9H); $^{13}C$ NMR (101 MHz, $CDCl_3$) δ 145.88, 141.77, 139.78, 129.15, 125.47, 123.55, 123.31, 122.57, 116.84, 114.86, 110.95, 77.46, 77.15, 76.83, 56.23, 40.26, 40.05, 30.31; Mass calculated for $C_{17}H_{20}N_4$: ESI m/z = 281.23. found 281.20; Elemental analysis: Anal. Calcd. for $C_{17}H_{20}N_4$: C, 72.83; H, 7.19; N, 19.98 %; Found: C, 72.81; H, 7.20; N, 19.96 %.

**2-(4-nitrophenyl)imidazo[1,2-a]pyridin-3-amine (1b)**

Brown solid; Yield: 84%; FT-IR (KBr, $cm^{-1}$): 3208 (NH); UV-Vis ($\lambda_{Max}$): 332 nm; $^1H$ NMR (400 MHz, $CDCl_3$) δ 8.33-8.22 (s, 1H), 8.20 (d, 2H), 8.11-8.09 (d, 1H), 7.69 (t, J = 8.9, 6.7, 1.4 Hz, 1H), 7.67 (d, 3H), 7.46 (s, 1H), 7.09 (s, 1H); $^{13}C$ NMR (101 MHz, $CDCl_3$) δ 157.71, 157.33, 147.22, 143.21, 139.36, 135.78, 127.85, 127.59, 124.48, 124.31, 117.52, 114.75, 114.15; Mass calculated for $C_{13}H_{10}N_4O_2$: ESI m/z = 254.08. found 254.76; Elemental analysis: Anal. Calcd. for $C_{13}H_{10}N_4O_2$: C, 61.41; H, 3.96; N, 22.04 %; Found: C, 61.40; H, 3.98; N, 22.05 %.

**2-(4-aminophenyl)imidazo[1,2-a]pyridin-3-amine (1c)**

Brown solid; Yield: 93%; FT-IR (KBr, $cm^{-1}$): 3400 (NH); UV-Vis ($\lambda_{Max}$): 314 nm; $^1H$ NMR (400 MHz, DMSO) δ 8.86 (d, J = 29.0 Hz, 1H), 8.22 (d, J = 7.3 Hz, 1H), 8.00 (t, J = 11.1 Hz, 2H), 7.96 – 7.85 (m, 2H), 7.81 (s, 1H), 7.69 (d, J = 7.6 Hz, 1H), 7.47 (s, 2H), 7.01 (t, J = 9.2 Hz, 1H), 6.99 – 6.57 (d, 2H); $^{13}C$ NMR (101 MHz, DMSO) δ 144.46, 136.11, 135.72, 135.27, 131.72, 128.13, 125.11, 116.51, 113.92, 112.52, 112.05; Mass calculated for $C_{13}H_{12}N_4$: ESI m/z = 224.10 found 224.06; Elemental analysis: Anal. Calcd. for $C_{13}H_{12}N_4$: C, 69.62; H, 5.39; N, 24.98 %; Found: C, 69.60; H, 5.40; N, 24.96 %.

**N-(tert-butyl)-2-(4-(dimethylamino)phenyl)imidazo[1,2-a]pyridin-3-amine (2)**

White solid; Yield: 93%; FT-IR (KBr, $cm^{-1}$): 3280 (NH); UV-Vis ($\lambda_{Max}$): 358 nm; $^1H$ NMR (400 MHz, $CDCl_3$) δ 8.21 (d, J = 7.8 Hz, 1H), 7.82 (d, J = 9.0 Hz, 2H), 7.54 (d, J = 9.0 Hz, 1H), 7.13 – 7.07 (m, 1H), 6.75 (d, J = 10.2 Hz, 2H), 3.13 (s, 1H), 2.99 (s, 6H), 1.06 (s, 9H);$^{13}C$ NMR (101 MHz, $CDCl_3$) δ 149.81, 141.61, 139.46, 128.90, 123.85, 123.33, 122.82, 122.44, 116.66, 112.10, 111.15, 56.32, 40.46, 30.39; Mass calculated for $C_{19}H_{24}N_4$: ESI m/z = 308.20 found 309.25 $(M + H)^+$; Elemental analysis: Anal. Calcd. for $C_{13}H_{12}N_4$: C, 73.99; H, 7.84; N, 18.17 %; Found: C, 73.96; H, 7.85; N, 18.18 %.

**2-(4-(dimethylamino)phenyl)imidazo[1,2-a]pyridin-3-amine (2a)**

Light brown solid; Yield: 90%; FT-IR (KBr, $cm^{-1}$): 3385 (NH); UV-Vis ($\lambda_{Max}$): 358 nm; $^1H$ NMR (400 MHz, DMSO) δ 8.18 (d, J = 6.7 Hz, 1H), 7.75 (d, J = 8.7 Hz, 2H), 7.61 (d, J = 9.0 Hz, 1H), 7.39 – 7.31 (m, 1H), 6.99 (t, J = 6.6 Hz, 1H), 6.81 (d, J = 8.8 Hz, 2H), 2.95 (s, 6H); $^{13}C$ NMR (101 MHz, DMSO) δ 157.75, 157.11, 150.62, 141.78, 127.89, 125.88, 123.90, 120.66, 116.87, 112.88, 112.54, 40.54, 40.38, 40.33, 40.13, 39.92, 39.71, 39.50, 39.29, 31.04; Mass calculated for $C_{15}H_{16}N_4$: ESI m/z = 252.13 found 253.11$(M + H)^+$; Elemental analysis: Anal. Calcd. for

$C_{15}H_{16}N_4$: C, 71.40; H, 6.39; N, 22.21 %; Found: C, 71.42; H, 6.40; N, 22.19 %.

The one-pot multicomponent production of the target components (**1-1c**) and (**2-2a**) was achieved with excellent yields. The formation of title compounds was characterized through HR-MS, FT-IR, UV-Vis, $^1$H NMR, $^{13}$C NMR, and elemental analysis. The complete spectroscopic characterization of compounds (**1-1c**) and (**2-2a**) was given in supporting information. The compound (**1**) was synthesized by the reaction of 4-nitrobenzaldehyde, 2-aminopyridine and tertiary butyl isocyanide in ethanolic medium by using iodine as a catalyst. Scheme 1 outlines the synthetic sequences of compound (**1**). The absorption spectra signify the characteristic peak at 368 nm. The peak at 33350 cm$^{-1}$ in the FT-IR spectra exposed the existence of amine moiety. The singlet peak at 8.25 ppm in the $^1$H NMR spectra indicates the existence of NH proton. The aromatic protons in the benzene ring were appeared at 8.18, 7.54 and 7.21 ppm respectively. The methyl protons of tertiary butyl group are appeared at a singlet in 1.09 ppm. The peak at 146.62 ppm in the $^{13}$C NMR spectra signifies the benzene carbon connected with $NO_2$ (-C-$NO_2$). The existence of tertiary butyl carbon was confirmed by the appearance of peak at 56.79 ppm. The methyl group carbons appeared at a peak at 30.48 ppm. The compound (**1**) showed base peak at m/z 310.20 in HR-MS spectra which matched well with their calculated molecular weight.

The compound (**1a**) was synthesized by the reaction of compound (**1**) by using Sn/HCl as a catalyst. Scheme 2 outlines the synthetic sequences of compound (**1a**). The absorption spectra signify the characteristic peak at 370 nm. The peak at 3315 cm$^{-1}$ in the FT-IR spectra displayed the existence of amine moiety. The singlet peak at 8.25 8.17 ppm in the $^1$H NMR spectra indicates the existence of NH proton. The aromatic protons in the benzene ring were appeared at 7.76 – 7.67, and 7.53 – 7.44, 7.09, ppm respectively. The methyl protons of tertiary butyl group are appeared at a singlet in 1.05 ppm. The peak at 145.88 ppm in the $^{13}$C NMR spectra signifies the benzene carbon connected with amine (-C-$NH_2$). The existence of tertiary butyl carbon was confirmed by the appearance of peak at 56.23 ppm. The methyl group carbons appeared at a peak at 30.31 ppm. The compound (**1a**) showed base peak at m/z 281.20 in HR-MS spectra which matched well with their calculated molecular weight.

The compound (**1b**) was synthesized by the reaction of compound (**1**) by using TFA.$H_2O$ (9:1) as a catalyst. Scheme 3 outlines the synthetic sequences of compound (**1b**). The absorption spectra signify the characteristic peak at 332 nm. The peak at 3208 cm$^{-1}$ in the FT-IR spectra exposed the attendance of amine moiety. The singlet peak at 8.33-8.20 ppm in the $^1$H NMR spectra indicates the existence of $NH_2$ proton. The aromatic protons in the benzene ring were appeared at 7.69 – 7.67, 7.46, and 7.09 ppm respectively. The peak at 157.71 ppm in the $^{13}$C NMR spectra signifies the benzene carbon connected with $NO_2$ (-C-$NO_2$). The existence of C=N moiety was confirmed by the appearance of peak at 147.32 ppm. The C=C carbons from pyridine nucleus appeared at a peaks at 114.75 and 114.15 ppm respectively. The compound (**1b**) showed base peak at m/z 254.76 in HR-MS spectra which matched well with their calculated molecular weight.

The compound (**1c**) was synthesized by the reaction of compound (**1b**) by using Sn/HCl as a catalyst. Scheme 4 outlines the synthetic sequences of compound (**1c**). The absorption spectra signify the characteristic peak at 314 nm. The peak at 3400 cm$^{-1}$ in the FT-IR spectra discovered the attendance of amine moiety. The singlet peak at 8.86 and 8.22 ppm in the $^1$H NMR spectra indicates the existence of $NH_2$ proton. The aromatic protons in the benzene ring were appeared at 8.00, 7.96-7.85 and 7.69 ppm respectively. The peak at 144.46 ppm in the $^{13}$C NMR spectra signifies the benzene carbon connected with amine (-C-$NH_2$). The existence of C=N moiety was confirmed by the appearance of peak at 136.11 ppm. The C=C carbons from pyridine nucleus appeared at a peaks at 135.72 and 135.27 ppm respectively. The compound (**1c**) showed base peak at m/z 224.06 in HR-MS spectra which matched well with their calculated molecular weight.

The compound (**2**) was produced by the reaction of N-dimethyl benzaldehyde, 2-aminopyridine and tertiary butyl isocyanide in ethanolic medium by using iodine as a catalyst. Scheme 5 outlines the synthetic sequences of compound (**2**). The absorption spectra signify the characteristic peak at 358 nm. The peak at 3280 cm$^{-1}$ in the FT-IR spectra discovered the occurrence of amine moiety. The singlet peak at 8.21 ppm in the $^1$H NMR spectra indicates the existence of NH proton. The aromatic protons in the benzene ring were appeared at 7.82, 7.54 and 7.13-7.07 ppm individually. The methyl protons from tertiary butyl group were confirmed by the peak at 1.06 ppm. The peak at 149.81 ppm in the $^{13}$C NMR spectra signifies the benzene carbon connected with N-dimethylamine (-C-$N(CH_3)_2$). The existence of C=N moiety was confirmed by the appearance of peak at 141.61 ppm. The C=C carbons from pyridine nucleus appeared at a peaks at 139.46 and 128.90 ppm respectively. The methyl carbon from N-dimethyl amine group was confirmed by the peak at 30.33 ppm. The compound (**2**) showed base peak at m/z 309.25 in HR-MS spectra which matched well with their calculated molecular weight.

The compound (**2a**) was synthesized by the reaction of compound (**2**) in TFA.$H_2O$ (9:1) as a catalyst. Scheme 6 outlines the synthetic sequences of compound (**2a**). The absorption spectra signify the characteristic peak at 358 nm. The peak at 3385 cm$^{-1}$ in the FT-IR spectra exposed the incidence of amine moiety. The singlet peak at 8.18 ppm in the $^1$H NMR spectra indicates the existence of $NH_2$ proton. The aromatic protons in the benzene ring were appeared at 7.75, 7.61 and 7.39-7.31 ppm respectively. The methyl proton from N-dimethyl amine group was confirmed by the peak at 2.95 ppm. The peak at 157.75 ppm in the $^{13}$C NMR

spectra signifies the benzene carbon connected with N-dimethylamine (-C-N($CH_3$)$_2$). The existence of C=N moiety was confirmed by the appearance of peak at 157.11 ppm. The C=C carbons from pyridine nucleus appeared at a peaks at 150.62 and 141.78 ppm respectively. The methyl carbon from N-dimethyl amine group was confirmed by the peak at 31.04 ppm. The compound (**2a**) showed base peak at m/z 253.11 in HR-MS spectra which matched well with their calculated molecular weight. The respective spectra of compounds (**1-1c**) and (**2-2a**) were presented in Figure. 2-23 .

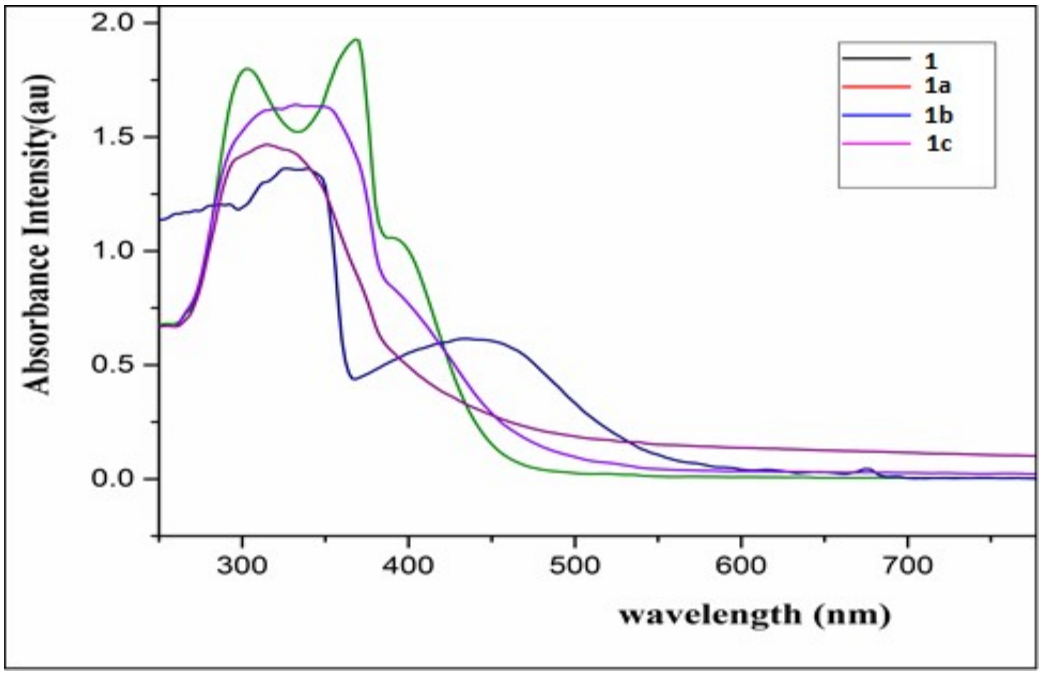


**Figure 2. UV-Vis spectra of compounds (1-1c)**

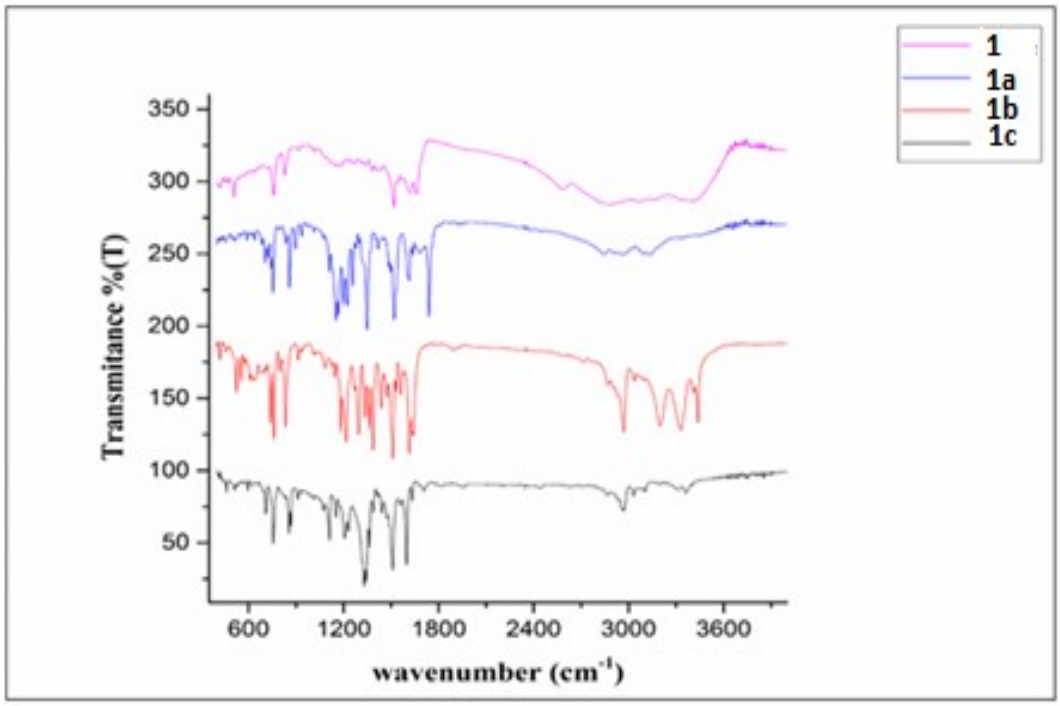


**Figure 3. FT-IR spectra of compounds (1-1c)**

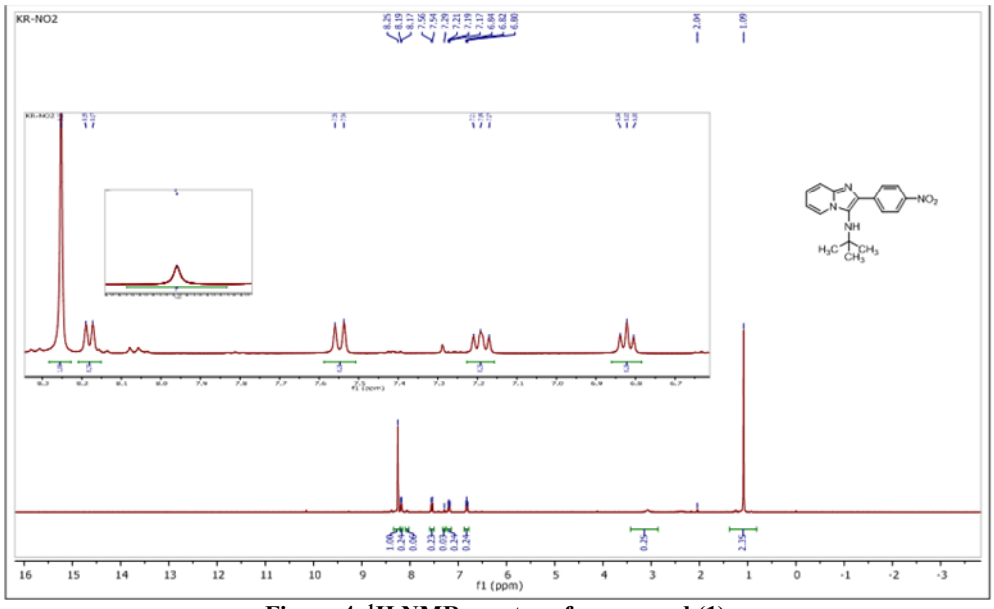


**Figure 4. $^{1}$H NMR spectra of compound (1)**

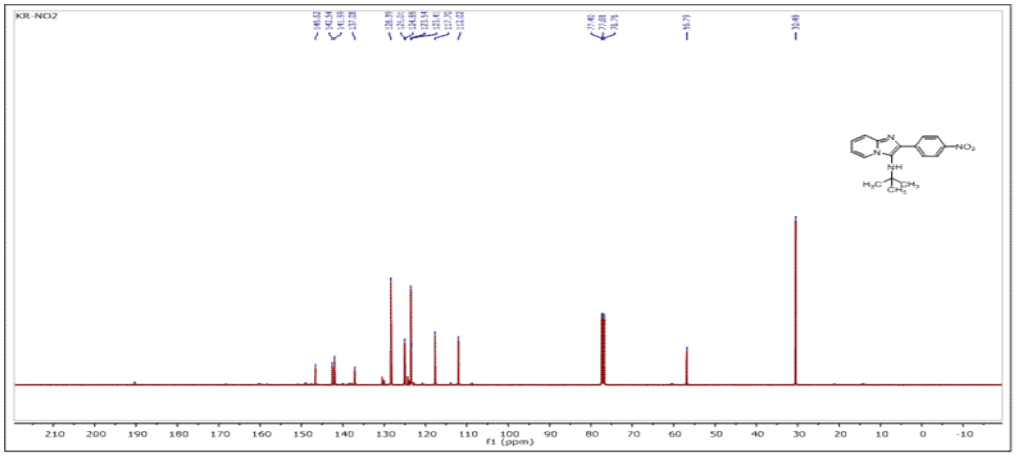


**Figure 5. $^{13}$C NMR spectrum of compound (1)**

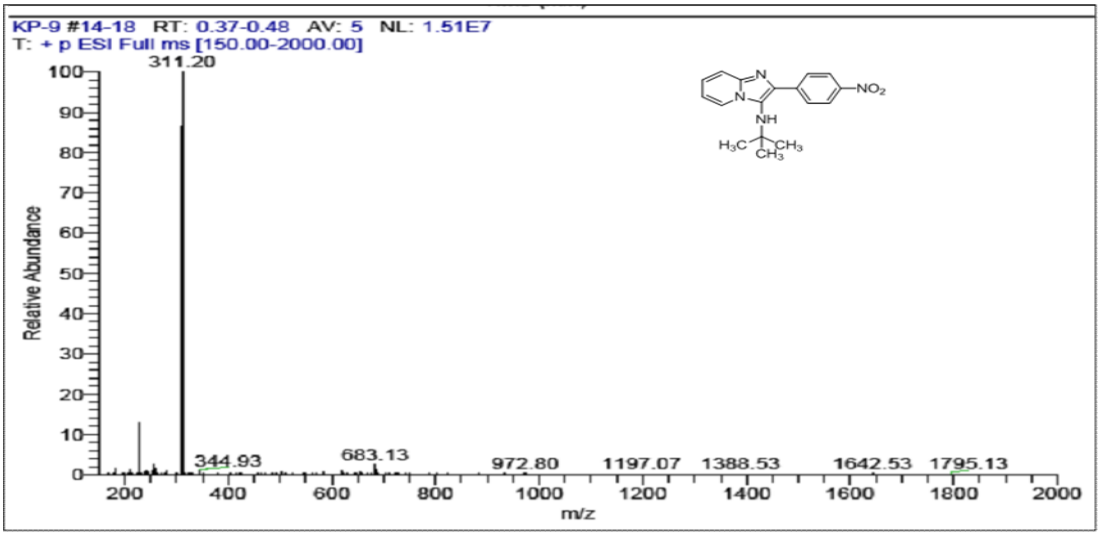


**Figure 6. HR-MS spectrum of compound (1)**

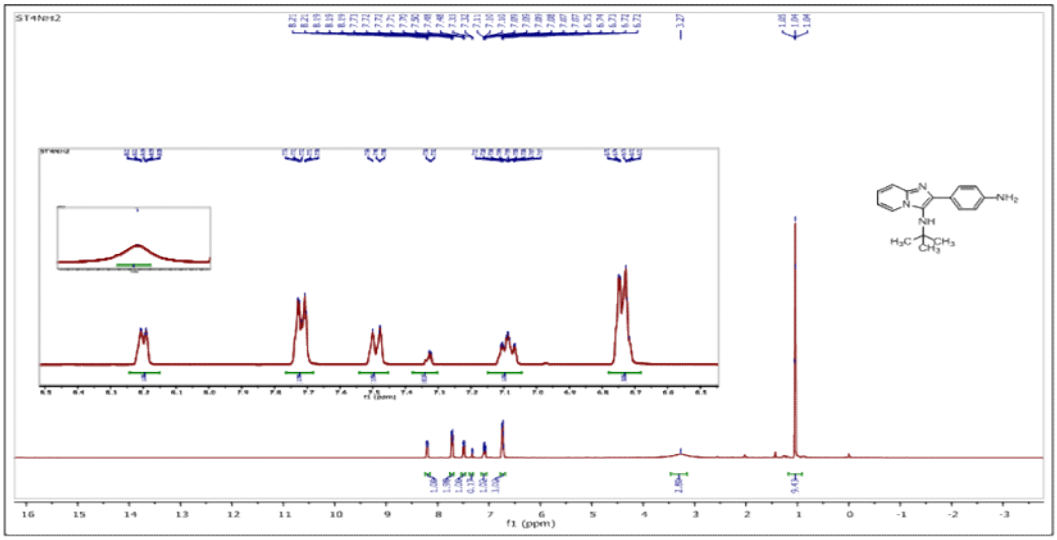

**Figure 7. $^{1}$H NMR spectra of compound (1a)**

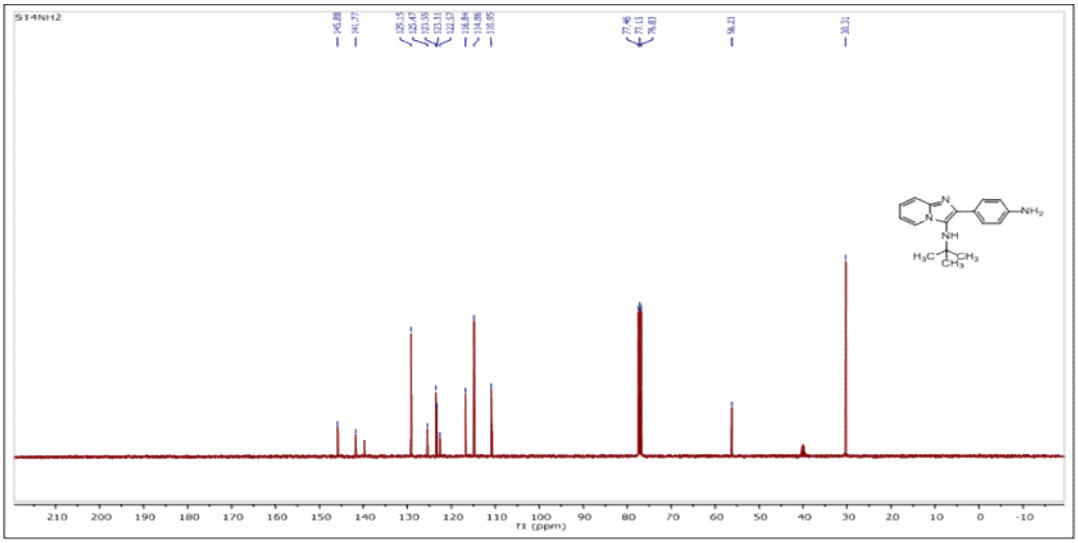

**Figure 8. $^{13}$C NMR spectrum of compound (1a)**

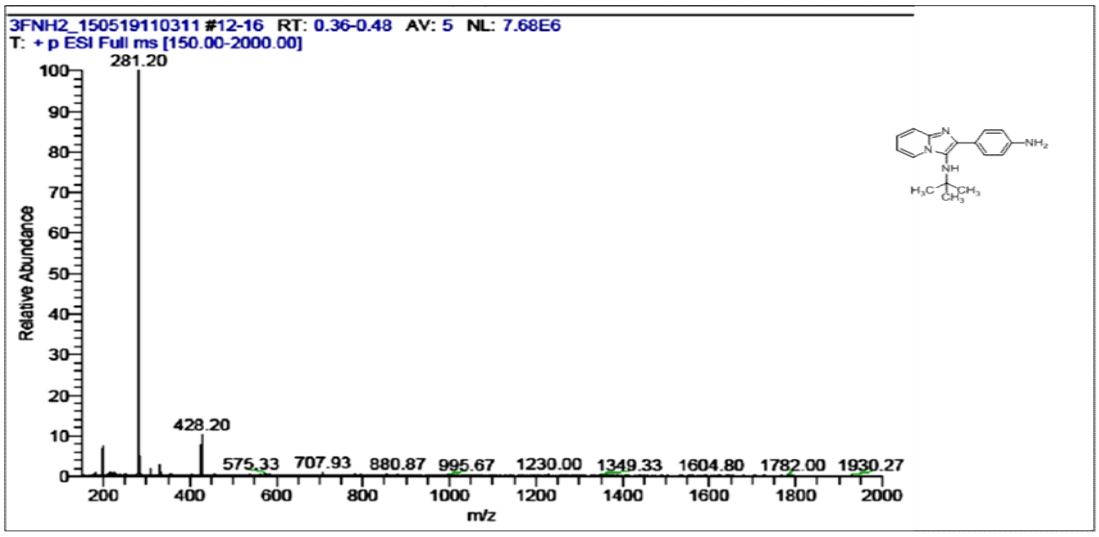


**Figure 9. HR-MS spectrum of compound (1a)**

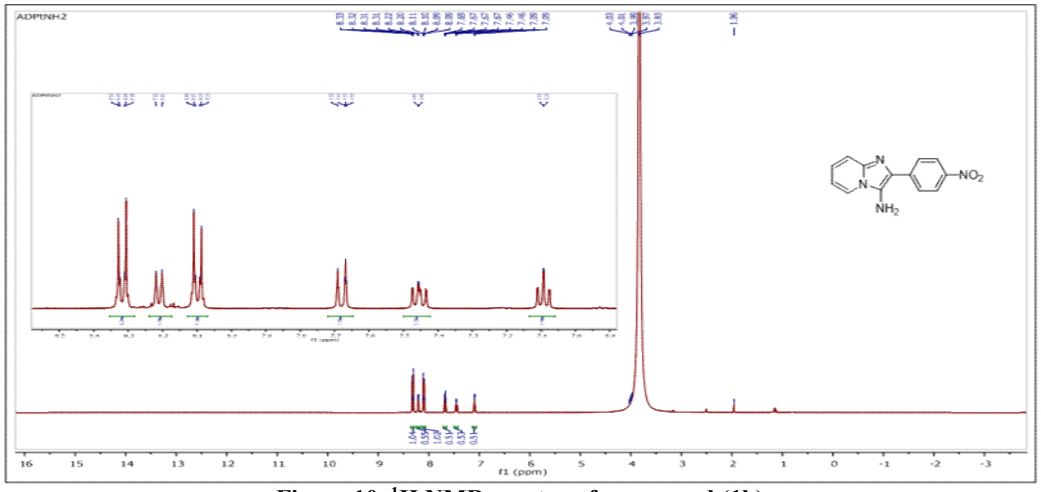


**Figure 10. $^{1}$H NMR spectra of compound (1b)**

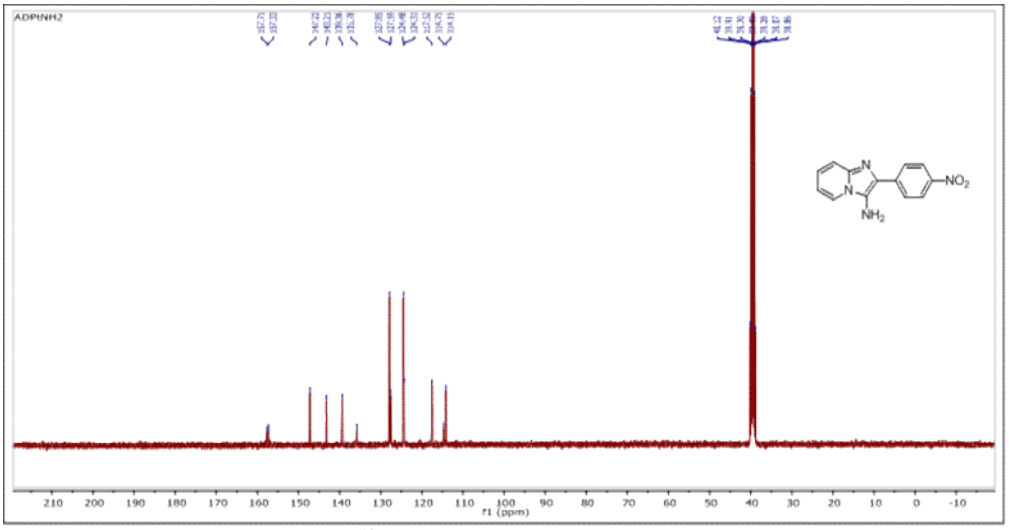


**Figure 11. $^{13}$C NMR spectrum of compound (1b)**

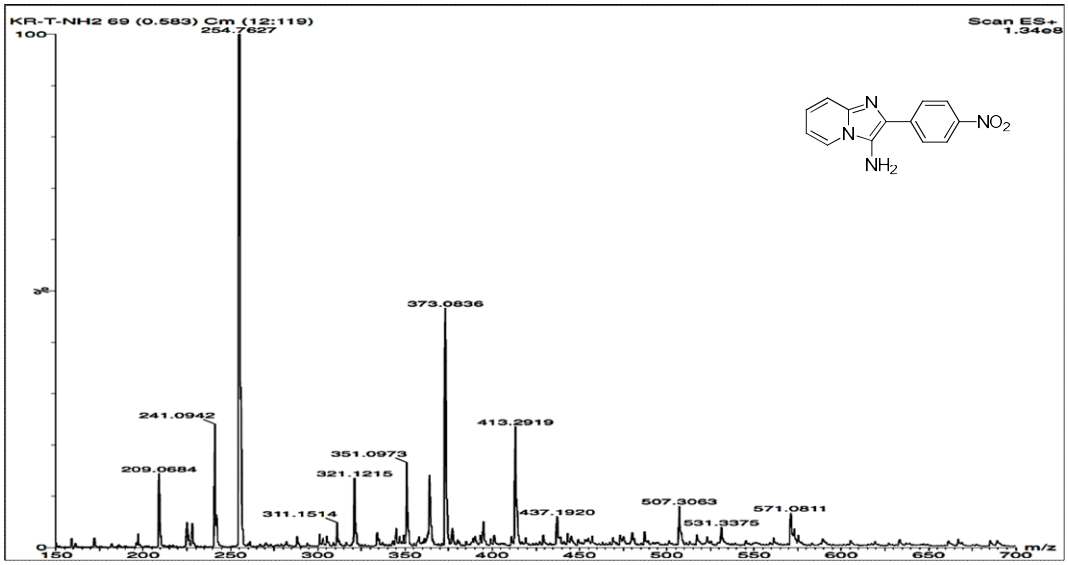


**Figure 12. HR-MS spectrum of compound (1b**

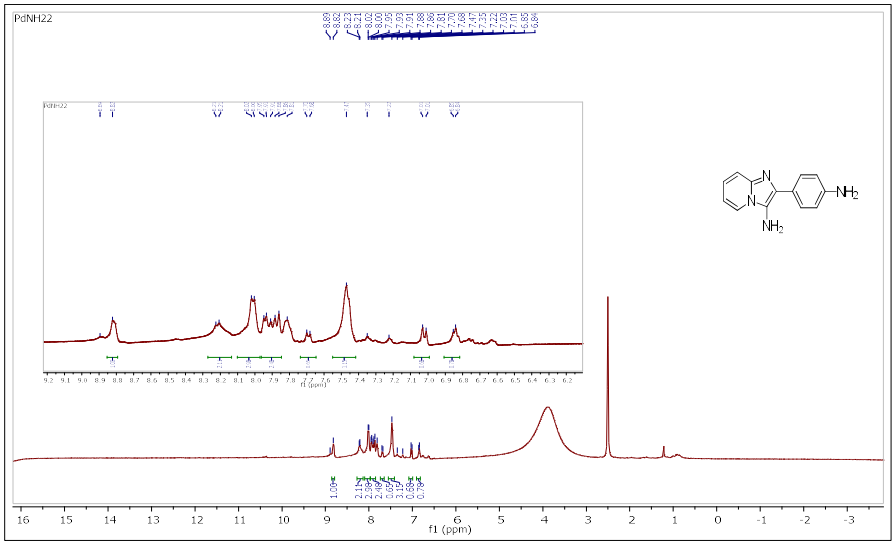


**Figure 13. $^{1}$H NMR spectra of compound (1c)**

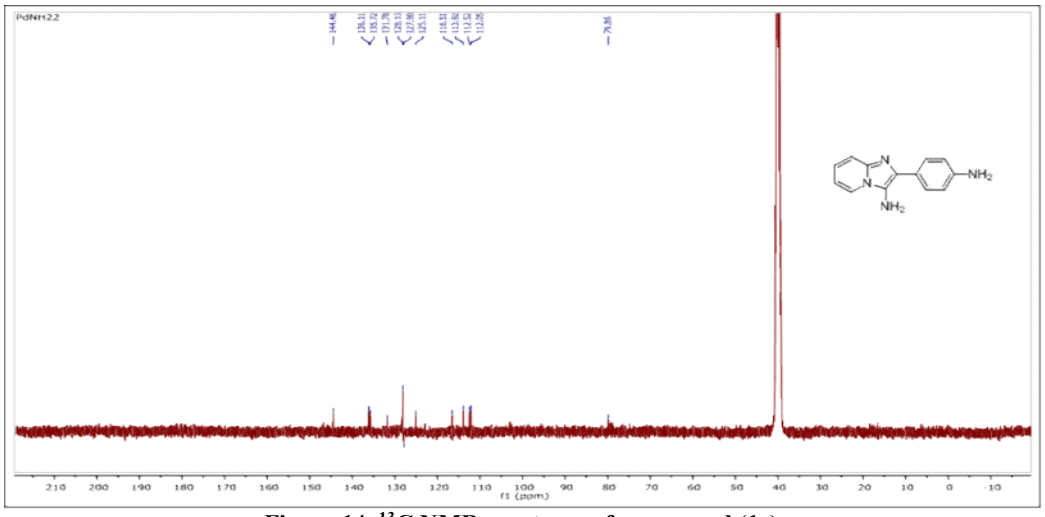


**Figure 14. $^{13}$C NMR spectrum of compound (1c)**

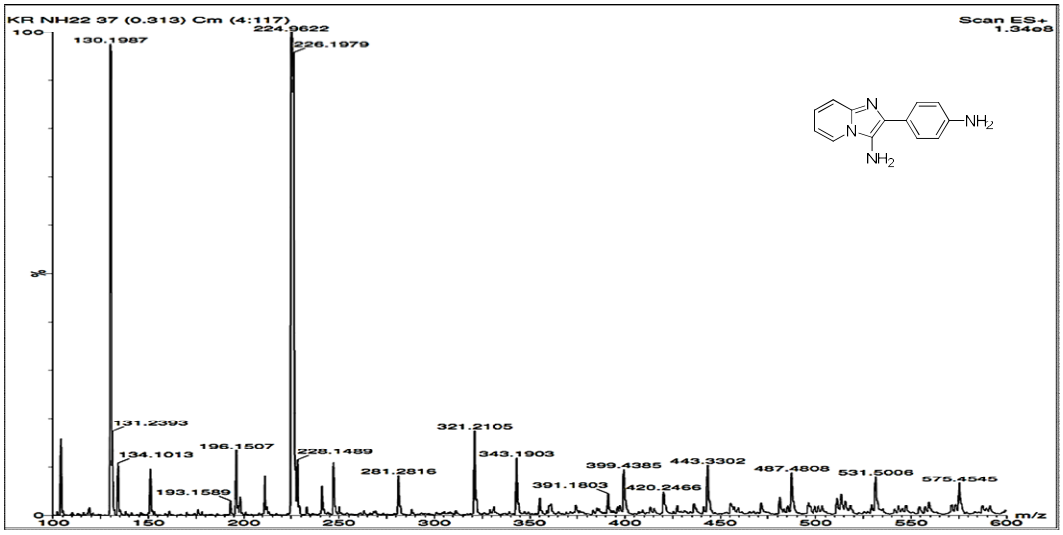


**Figure 15. HR-MS spectrum of compound (1c)**

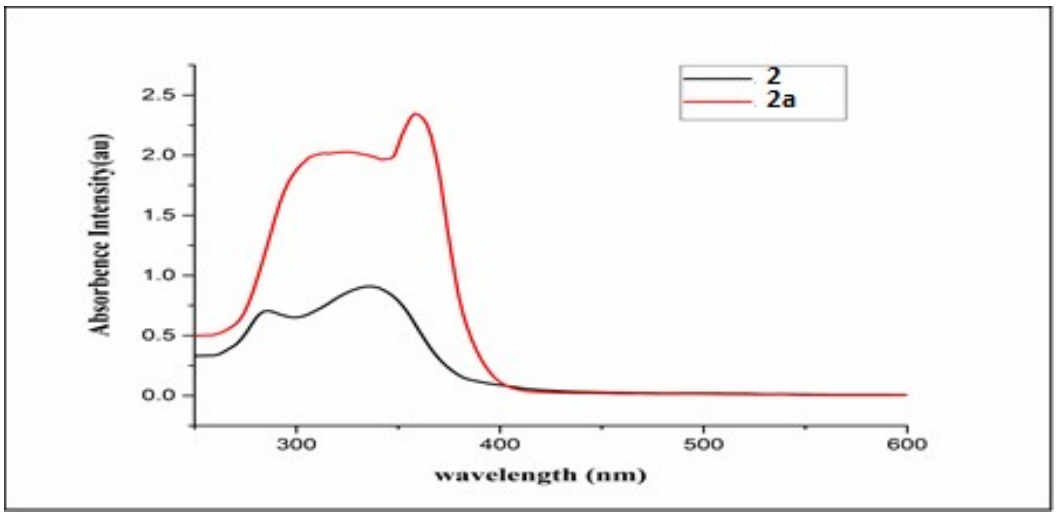


**Figure 16. UV-Vis spectra of compounds (2-2a)**

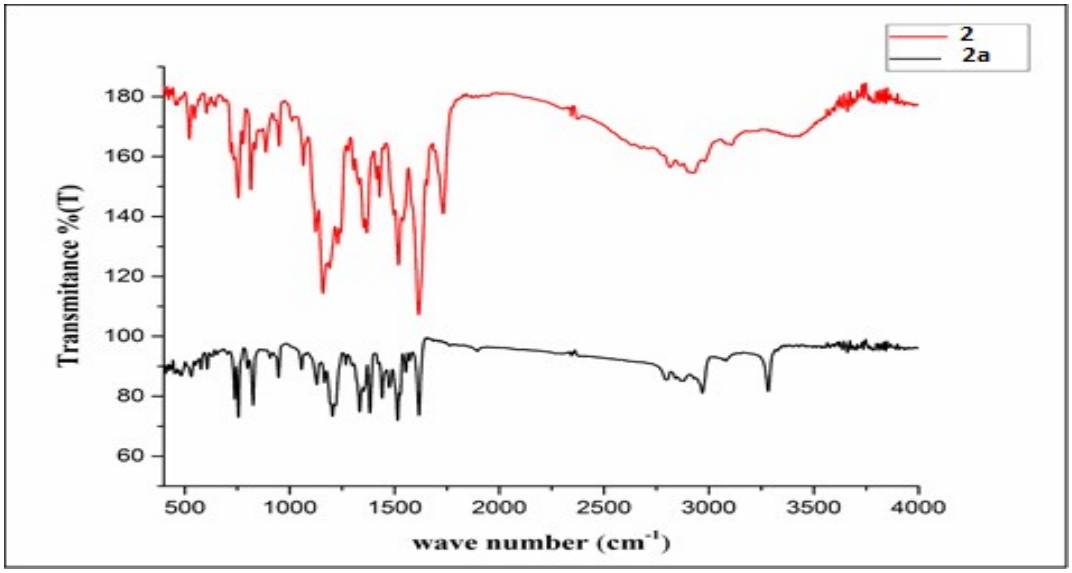


**Figure 17. FT-IR spectra of compounds (2-2a)**

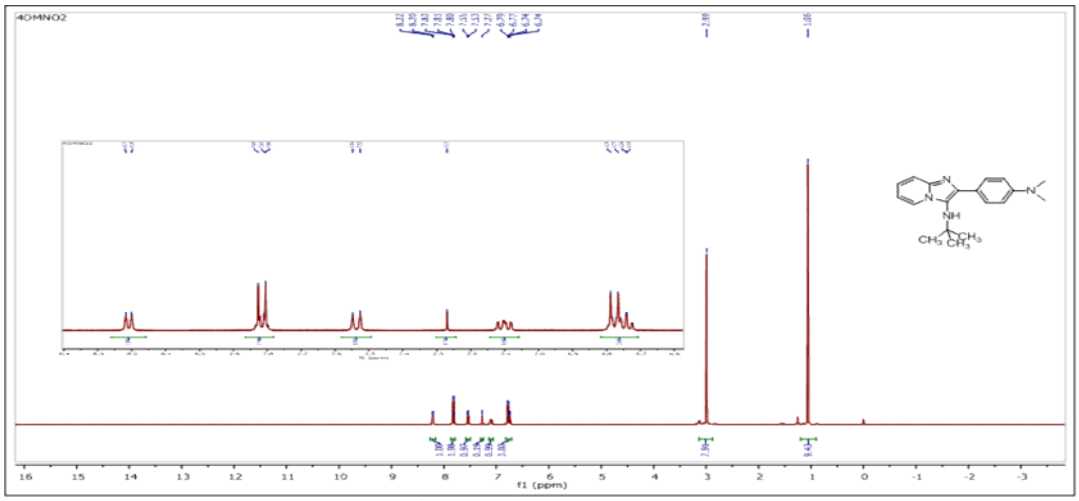


**Figure 18. $^{1}$H NMR spectra of compound (2)**

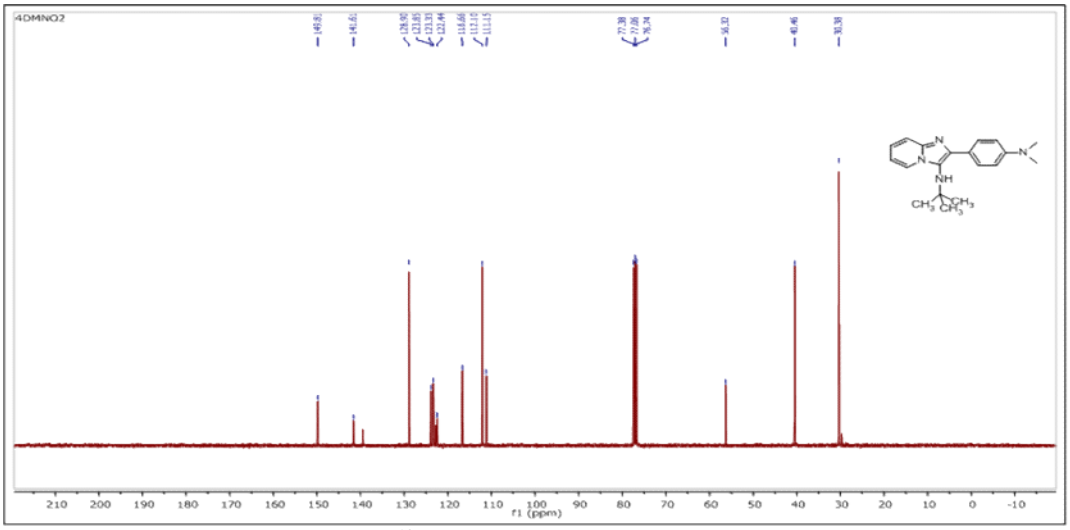


**Figure 19. $^{13}$C NMR spectrum of compound (2)**


**Figure 20. HR-MS spectrum of compound (2)**

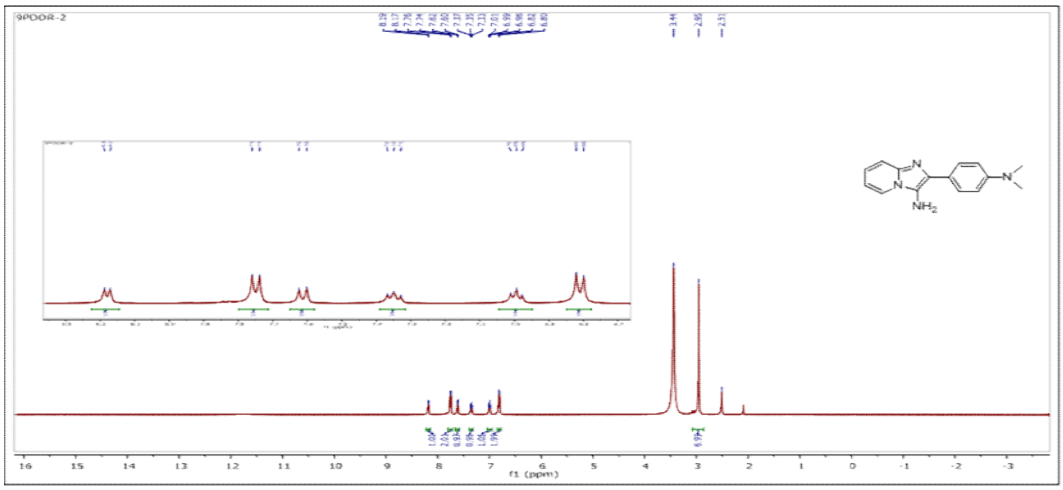


**Figure 21. $^{1}$H NMR spectra of compound (2a)**

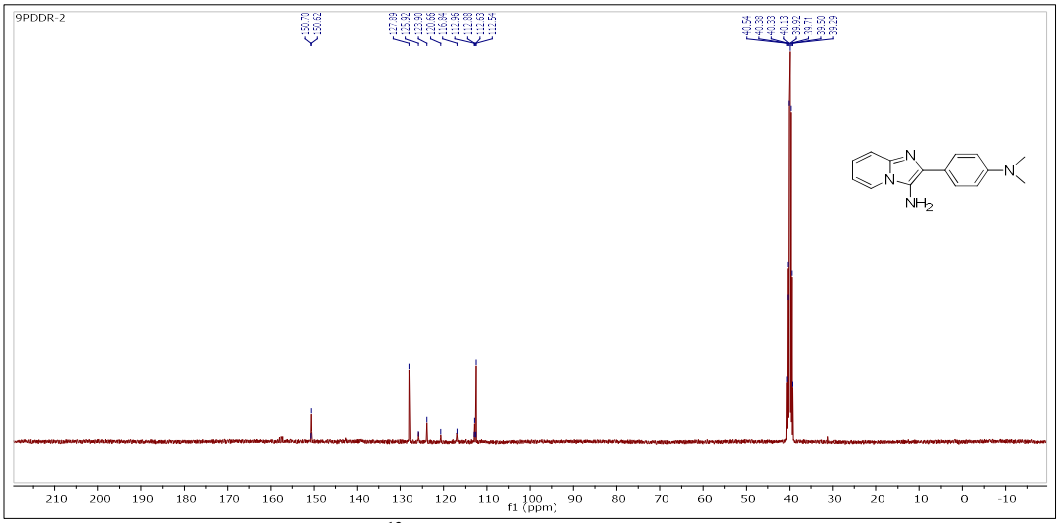


**Figure 22. $^{13}$C NMR spectrum of compound (2a)**

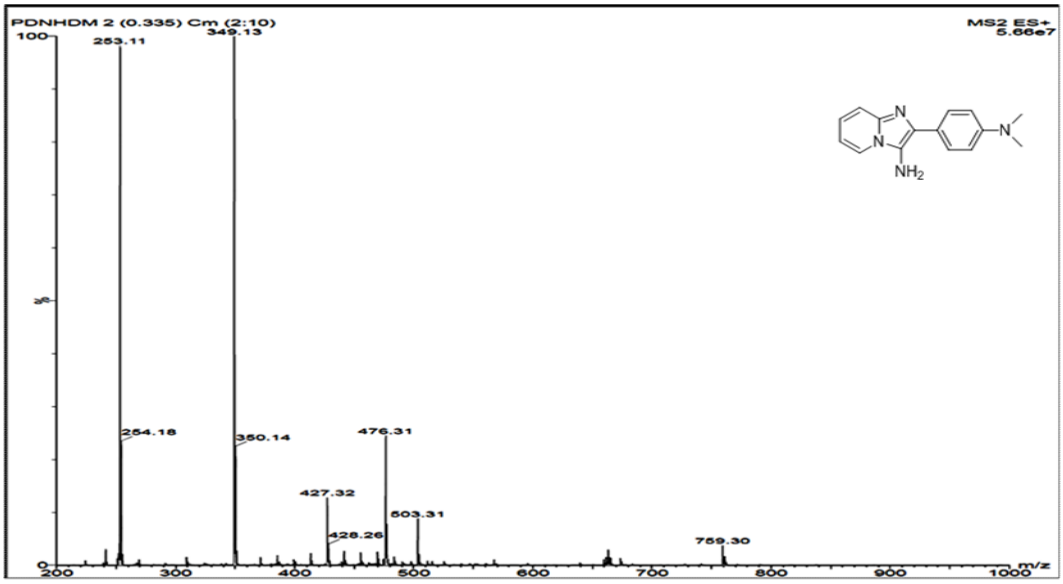


**Figure 23. HR-MS spectrum of compound (2a)**

**Antidiabetic activity**

**α-Glucosidase assay**

The inhibiting effects of the analogues (**1-1c**) and (**2-2a**) on α-glucosidase were examined. The current study demonstrated that the synthesized compounds (**1-1c**) and (**2-2a**) exhibited inhibitory action towards α-glucosidase, with $IC_{50}$ values 165.59 to 370.63 µM, except for compounds **1**, **1b**, and **2**, which had $IC_{50}$ values of 325.81, 270.35, and 370.63 µM, individually, in contrast to the standard acarbose ($IC_{50}$ = 260.21 µM). The substances (**1a** and **1c**), having $IC_{50}$ values of 165.59 and 169.37 µM correspondingly, demonstrated significant antidiabetic effects associated to the standard acarbose, which has an $IC_{50}$ value of 260.21 µM. Only compound (**2**) exhibited diminished antidiabetic efficacy, having $IC_{50}$ value of 370.63 µM, in comparison to the standard acarbose ($IC_{50}$ = 260.21 µM). The results were summarized in Table 1.

**Table 1. Antidiabetic effect of compounds (1-1c) and (2-2a) through α-Glucosidase inhibition assay**

| Compound | Inhibition rate (%) | | | | $IC_{50}$ (µM) |
|---|---|---|---|---|---|
| | 125 (µM) | 250 (µM) | 500 (µM) | 1000 (µM) | |
| **1** | 24.2 ±1.8 | 44.3 ±2.7 | 80.6 ±0.4 | 96.3 ±1.7 | 325.81 |
| **1a** | 38.2 ±2.3 | 52.6 ±0.4 | 92.5 ±1.5 | 96.7 ±0.3 | 165.59 |

| | | | | | |
|---|---|---|---|---|---|
| **1b** | 28.5 ±1.2 | 48.3 ±2.7 | 86.2 ±1.5 | 94.5±0.5 | 270.35 |
| **1c** | 40.2 ±0.8 | 58.5 ±1.5 | 72.3 ±1.7 | 86.4 ±2.6 | 169.37 |
| **2** | 30.2 ±2.8 | 42.5 ±0.5 | 64.6 ±1.4 | 88.2 ±1.8 | 370.63 |
| **2a** | 34.2 ±2.5 | 58.2 ±0.8 | 78.6 ±1.4 | 92.2 ±2.8 | 205.36 |
| **Acarbose** | 36.2 ±0.7 | 48.4 ±1.6 | 75.8 ±2.2 | 94.4 ±1.6 | 260.21 |

**α-amylase assay**

In Table 2, the α-amylase inhibitory nature of the compounds (**1-1c**) and (**2-2a**) are exhibited. The outcomes prove that the produced compounds display superior action than control acarbose. Nevertheless, the inhibitory nature of all the synthesized compounds (**1-1c**) and (**2-2a**) is dependent on concentration. Most of the synthesized compounds (**1-1c**) and (**2-2a**) displayed significant antidiabetic potential except compounds **1**, **1b**, and **2** with the $IC_{50}$ values of 365.22, 240.16, and 324.55 µM. Of the synthesised compounds (**1-1c**) and (**2-2a**), compound (**1a**) revealed significant effect ($IC_{50}$ = 141.28 µM) associated to the reference acarbose ($IC_{50}$ = 188.00 µM). The compound **1** ($IC_{50}$: 365.22 µM) had a moderate antidiabetic action, then the standard acarbose ($IC_{50}$: 188.00 µM).

**Table 2. Antidiabetic effect of compounds (1-1c) and (2-2a) through α-amylase inhibition action**

| Compound | Inhibition rate (%) | | | | $IC_{50}$ (µM) |
|---|---|---|---|---|---|
| | 125 (µM) | 250 (µM) | 500 (µM) | 1000 (µM) | |
| **1** | 30.5 ±2.5 | 49.2 ±1.8 | 62.4 ±0.6 | 78.6 ±1.4 | 365.22 |
| **1a** | 42.7 ±1.3 | 58.8 ±2.2 | 76.1±1.9 | 92.8 ±0.2 | 141.28 |
| **1b** | 43.2 ±0.8 | 51.8 ±1.2 | 63.2 ±2.8 | 91.9 ±1.1 | 240.16 |
| **1c** | 42.1 ±1.9 | 60.2 ±0.5 | 73.5±1.5 | 92.7 ±2.3 | 146.93 |
| **2** | 28.2 ±2.8 | 44.8 ±1.2 | 74.9 ±1.1 | 94.5±0.3 | 324.55 |
| **2a** | 37.0 ±1.5 | 59.1 ±2.9 | 80.2 ±1.8 | 95.0 ±0.8 | 175.83 |
| **Acarbose** | 32.9 ±2.1 | 58.3 ±1.7 | 87.2 ±0.6 | 96.8±1.2 | 188.00 |

## CONCLUSION

In summary, we have devised a novel, effective, one-pot multi-component procedure to synthesize imidazo[1,2-a]pyridine analogues (**1-1c**) and (**2-2a**) that have possible structural and therapeutic significance. We utilized numerous Lewis's acids as catalysts for the production of the title substances. The combination of 2-aminopyridine, tert-butyl isocyanide, and substituted benzaldehyde in the presence of iodine as a catalyst yield compounds **1** and **2**. The compounds (**1** and **2**) were further reduced to get their analogues (**1a-1c**) and (**2a**). The imidazo-pyridine analogues were studied by UV-Vis, FT-IR, NMR, mass spectrometry, and elemental analysis. The primary benefits of this procedure are the exceptional yielding of the goods and the utilization of uncomplicated beginning resources. The technique's efficiency renders it an appealing substitute to different methods. The compounds (**1-1c**) and (**2-2a**) were assessed for their in-vitro antidiabetic activities. Several of the formulated compounds exhibited remarkable antidiabetic efficacy comparable to the conventional medication acarbose. The experimental results indicate that imidazo[1,2-a]pyridine analogues serve as a promising framework for the creation of novel bioactive compounds. Additional inquiries including comprehensive mechanistic research, extensive biological assessments, and structure–activity connection evaluations are necessary to thoroughly investigate their clinical efficacy.

## REFERENCES


1. Dutta BJ, Singh S, Seksaria S, Gupta GD, Singh A. Inside the diabetic brain: Insulin resistance and molecular mechanism associated with cognitive impairment and its possible therapeutic strategies. Pharmacol. Res. 2022;182:106358.
2. Gupta A, Jamal A, Jamil DA, Al-Aubaidy HA. A systematic review exploring the mechanisms by which citrus bioflavonoid supplementation benefits blood glucose levels and metabolic complications in type 2 diabetes mellitus. Diabetes Metab. Syndr. 2023;17(11):102884.
3. Taha M, Khan AA, Rahim F, Hayat S, Imran S, Iqbal N, Uddin N, Khan KM, Anouar EH, Farooq RK, Nawaz M. Synthesis, in vitro evaluation and molecular docking studies of hybrid 4-quinolinyl bearing 1, 3, 4-thiadiazole-2-amine as a new inhibitor of α-amylase and α-glucosidase. J. Mol. Struct. 2023;1282:135173.
4. Santos CM, Freitas M, Fernandes E. A comprehensive review on xanthone derivatives as α-glucosidase inhibitors. Eur. J. Med. Chem. 2018;157:1460–1479.
5. Taha M, Hayat S, Rahim F, Uddin N, Wadood A, Nawaz M, Gollapalli M, Rehman AU, Khan KM, Farooq RK. Exploring thiazole-based Schiff base analogs as potent α-glucosidase and α-amylase inhibitor: their synthesis and in-silico study. Bioorg. Chem. 2023;1287:135672.
6. Imran S, Taha M, Selvaraj M, Ismail NH, Chigurupati S, Mohammad JI. Synthesis and biological evaluation of indole derivatives as α-

amylase inhibitor. Bioorg. Chem. 2017;73:121–127.
7. Kazempour-Dizaji M, Mojtabavi S, Sadri A, Ghanbarpour A, Faramarzi MA, Navidpour L. Arylureidoaurones: Synthesis, in vitro α-glucosidase, and α-amylase inhibition activity. Bioorg. Chem. 2023;139:106709.
8. Agarwal A, Srivastava K, Puri SK, Chauhan PM. Antimalarial activity and synthesis of new trisubstituted pyrimidines. Bioorg. Med. Chem. Lett. 2005;15(12):3130–3132.
9. Gupta A, Bhat HR, Singh UP. Discovery of novel hybrids of Morpholino-1, 3, 5-triazine-pyrimidine as an anti-diabetic agent in High-fat, Low-dose Streptozotocin-induced diabetes in Wistar rats: an in-vitro, in-silico and in-vivo study. J. Mol. Struct. 2023;1294:136478.
10. Zhu J, Bienaymé H, editors. Multicomponent Reactions. Weinheim: Wiley-VCH; 2005.
11. Basso A, Banfi L, Riva R, Guanti G. Novel utilization of multicomponent reactions. J. Org. Chem. 2005;70(2):575–579.
12. Ramon DJ, Yus M. Asymmetric multicomponent reactions (AMCRs): The next frontier. Angew. Chem. Int. Ed. Engl. 2005;44(11):1602–1634.
13. Dömling A. Recent advances in isocyanide-based multicomponent reactions. Chem. Rev. 2006;106(1):17–89.
14. Shukla NM, Salunke DB, Yoo E, Mutz CA, Balakrishna R, David SA. Antibacterial activities of Groebke–Blackburn–Bienaymé-derived imidazo [1,2-a] pyridin-3-amines. Bioorg. Med. Chem. 2012;20(19):5850–5863.
15. Al-Tel TH, Al-Qawasmeh RA. Post Groebke–Blackburn multicomponent protocol: synthesis of new polyfunctional imidazo [1,2-a] pyridine and imidazo [1,2-a] pyrimidine. Eur. J. Med. Chem. 2010;45(12):5848–5855.
16. Starrett JE Jr, Montzka TA, Crosswell AR, Cavanagh RL. Synthesis and biological activity of 3-substituted imidazo [1,2-a] pyridines as antiulcer agents. J. Med. Chem. 1989;32(9):2204–2210.
17. Mirmashhori B, Azizi N, Saidi MR. A simple, economical, and highly efficient synthesis of β-hydroxynitriles from epoxide under solvent free conditions. J. Mol. Catal. A Chem. 2006;247(1-2):159–161.
18. Gueiffier A, Mavel S, Lhassani M, Elhakmaoui A, Snoeck R, Andrei G, Chavignon O, Teulade JC, Witvrouw M, Balzarini J. Synthesis of imidazo [1, 2-a] pyridines as antiviral agents. J. Med. Chem. 1998;41(25):5108–5112.
19. Langer SZ, Arbilla S, Benavides J, Scatton B. Zolpidem and necopidem: two imidazopyridines with selectivity for omega 1 and omega 3 receptor subtypes. Psychopharmacology. 1990;102(1):61–72.
20. Boerner RJ, Möller HJ. The importance of new antidepressants in the treatment of anxiety/depressive disorders. Pharmacopsychiatry. 1999;32(4):119–126.
21. Boggs S, Elitzin VI, Gudmundsson K, Martin MT, Sharp MJ. Kilogram-scale synthesis of the CXCR4 antagonist GSK812397. Org. Process Res. Dev. 2009;13(4):781–785.
22. Jenkinson S, Thomson M, McCoy D, Edelstein M, Danehower S, Lawrence W, Wheelan P, Spaltenstein A, Gudmundsson K. Blockade of X4-tropic HIV-1 cellular entry by GSK812397, a potent noncompetitive CXCR4 receptor antagonist. Antimicrob. Agents Chemother. 2010;54(2):817–824.
23. Choi WT, Duggineni S, Xu Y, Huang Z, An JJ. Drug discovery research targeting the CXC chemokine receptor 4 (CXCR4). J. Med. Chem. 2012;55(3):977–994.
24. Enguehard-Gueiffier C, Gueiffier A. Recent progress in the pharmacology of imidazo[1,2-a]pyridines. Mini Rev. Med. Chem. 2007;7(9):888–899.
25. Katritzky AR, Xu YJ, Tu H. Regiospecific synthesis of 3-substituted imidazo [1, 2-a] pyridines, imidazo [1, 2-a] pyrimidines, and imidazo [1, 2-c] pyrimidine. J. Org. Chem. 2003;68(12):4935–4937.
26. Blackburn C. A three-component solid-phase synthesis of 3-aminoimidazo [1, 2-a] azines. Tetrahedron Lett. 1998;39(31):5469–5472.
27. Blackburn C, Guan B. A novel dealkylation affording 3-aminoimidazo [1, 2] pyridines: access to new substitution patterns by solidphase synthesis. Tetrahedron Lett. 2000;41(10):1495–1500.
28. Bagdi AK, Santra S, Monir K, Hajra A. Synthesis of imidazo[1,2-a]pyridines: a decade update. Chem.Commun. 2015;51(85):1555–1575.
29. Mandair GS, Light M, Russell A, Hursthouse M, Bradley M. Re-evaluation of the outcome of a multiple component reaction—2- and 3-amino-imidazo[1,2-a]pyrimidines? Tetrahedron Lett. 2002;43(23):4267–4269.
30. Rousseau AL, Matlaba P, Parkinson CJ. Multicomponent synthesis of imidazo[1,2-a]pyridines using catalytic zinc chloride. Tetrahedron Lett. 2007;48(23):4079–4082.
31. Aroua LM, Almuhaylan HR, Alminderej FM, Messaoudi S, Chigurupati S, Al-Mahmoud S, Mohammed HA. Synthesis and biological evaluation of new imidazole derivatives. Bioorg. Chem. 2021;114:105073.
32. Martin AE, Montgomery PA. Acarbose: An alpha-glucosidase inhibitor. Am. J. Health Syst. Pharm. 1996;53(19):2277–2287.
33. Yousuf S, Khan KM, Salar U, Chigurupati S, Muhammad MT, Wadood A, Aldubayan M, Vijayan V, Riaz M, Perveen S. Synthesis, in vitro evaluation, and molecular docking studies of new derivatives as potent enzyme inhibitors. Eur. J. Med. Chem. 2018;159:47–72.

34. Saleem F, Khan KM, Chigurupati S, Solangi M, Nemala AR, Mushtaq M, Ul-Haq Z, Taha M, Perveen S. Synthesis and evaluation of new bioactive molecular hybrids. Bioorg, Chem. 2021;106:104489.